ORIGINAL PAPER

Developing an innovative and high-performance method for recovering reusable launcher stages: the in-air capturing method

S. Stappert[1] · S. Singh[1] · A. Funke[2] · M. Sippel[1]

Abstract

In this paper, the research within the Horizon 2020-funded project FALCon on the innovative "In-Air Capturing" (IAC) method is presented. This recovery method for reusable rocket stages involves capture of a winged launcher stage with an aircraft in a gliding flight at subsonic velocity. Hence, the IAC procedure involves multiple vehicles interacting in a highly dynamic and complex environment, which requires detailed investigation before being used in a future full-scale setup. First, this paper gives an overview of the implications of using the IAC method on launcher system design. Second, the subscale flight testing with unmanned aerial systems (UASs) is explained. An analysis of all full-scale systems involved is also conducted, including the towing aircraft, an aerodynamically controlled capturing device that is connected via a rope to the aircraft, and the RLV stage. CFD simulations are conducted to understand the implications of the flow field around the vehicles and their impact on the IAC maneuver. Next, some full-scale trajectory simulations for different maneuvers involved in IAC are produced. The trajectory is also evaluated for subscale flight simulations, wherein the data acquired during flight tests is used. Finally, the progress and potential future outlook for this recovery method are described.

Abbreviations

ACCD	Aerodynamically controlled capturing device
AoA	Angle of attack
BVLOS	Beyond visual line of sight
CFD	Computational fluid dynamics
DOF	Degrees of freedom
DRL	Downrange landing
FALCon	Formation flight for in-air launcher 1st stage capturing demonstration
FB	Flyback
FPA	Flight path angle
GTO	Geosynchronous transfer orbit
GLOM	Gross lift-off mass
IAC	In-air capturing
IRL	Integration readiness level
IMR	Inert mass ratio
L/D	Lift to drag
MECO	Main engine cutoff

MTOW	Maximum take-off weight
RANS	Reynolds-averaged Navier–Stokes
RLV	Reusable launch vehicle
RLVD	Reusable launch vehicle demonstrator
RTLS	Return to launch site
TA	Towing aircraft
TAD	Towing aircraft demonstrator
TRL	Technology readiness level
UA	Unmanned aircraft
UAS	Unmanned aerial system
VTHL	Vertical take-off, horizontal landing
VTVL	Vertical take-off, vertical landing

✉ S. Singh
sunayna.singh@dlr.de

[1] DLR, Institute of Space Systems, Bremen, Germany

[2] DLR, Institute of Flight Systems, Brunswick, Germany

1 Introduction

The idea of reusing launch vehicles (RLVs), or parts of it, is almost as old as space flight itself. Recovering and reusing complete stages could lower launch costs, minimize the environmental impact of rocket launches and, subsequently, enable low-cost space transportation with high launch rates. Thus, reusability has the potential to be a serious game changer in space transportation, as also successfully proven by SpaceX with the Falcon 9. It is logically a crucial matter

to investigate the means of recovering and RLV stages for a possible future generation of European launch vehicles.

Even before SpaceX proved the viability of their vertical landing concept with the Falcon 9, RLVs have been studied at DLR [1–3]. In the wake of these studies, a highly innovative and performant method for recovery of returning rocket stages was invented: the in-air capturing (IAC) method [3, 5]. This method is based on the idea of using aerodynamic forces only to decelerate the winged returning stage. After reaching subsonic velocity and entering a steady gliding flight, comparable to the Space Shuttle Orbiter, a suitable aircraft towing a capturing device via a rope would match the stage's velocity and flight path angle (FPA) and capture the stage. Once the connection is established, the stage would be towed back to the landing site where it lands automatically. Figure 1 shows the artist's impression of the IAC maneuver.

In the past few years, DLR has initiated extensive research on this recovery method. The DLR in-house project AKIRA [4] was a starting point which led to the EU-funded Horizon 2020 project FALCon (Formation flight for in-Air Launcher 1st stage Capturing demonstration). FALCon involved DLR, together with a range of European companies and academic institutions. In this project, the technologies that are necessary for a future full-scale IAC demonstration have been investigated. The goal is to advance the IAC technology with full-scale simulations and subscale flight tests. Part of the results of this analysis are shown in the paper. First, the IAC method is explained and a roadmap toward its development

is presented. The subscale demonstration of the IAC maneuver with unmanned aerial systems (UASs) is explained in Sect. 3. Then, the full-scale vehicles involved in the procedure are explained in detail in Sect. 4. Some critical subsystems that affect the dynamics of the full-scale scenario are also briefly presented. Finally, in Sect. 5, the simulation results for both full-scale and subscale IAC are evaluated. The paper concludes with an outlook onto the future path of developing this highly performant and innovative return method.

2 In-air capturing method

The IAC method was invented and patented at DLR in 2003 [6]. A schematic of a typical IAC mission is shown in Fig. 2. The launch vehicle takes off vertically like a conventional launcher. After main engine cutoff (MECO), the RLV stage separates from the rest of the launcher and travels along a ballistic, suborbital trajectory. Once the denser parts of the atmosphere are entered, the aerodynamic forces start to build up and allow the deceleration of the stage by lift and drag forces. To minimize the loads on the stage, the magnitude of the forces has to be controlled. At subsonic velocity, the RLV stage enters a state of equilibrium gliding flight with almost constant velocity and flight path angle (FPA), similar to the Space Shuttle Orbiter's final approach. Once an altitude of 10 km is reached, the towing aircraft (TA) already awaits the returning stage and enters a diving flight to match position, velocity and heading of the RLV stage. Once a mechanical connection is established through the aerodynamically controlled capturing device (ACCD), the TA starts to tow the stage back to a landing site. There, the stage disconnects from the ACCD and conducts an autonomous, horizontal landing which marks the end of the mission.

Hence, the IAC method features three different vehicles: the returning RLV stage, the TA and the ACCD. Each of those has a unique set of requirements and tasks. The TA needs to have the capability to match the RLV's gliding
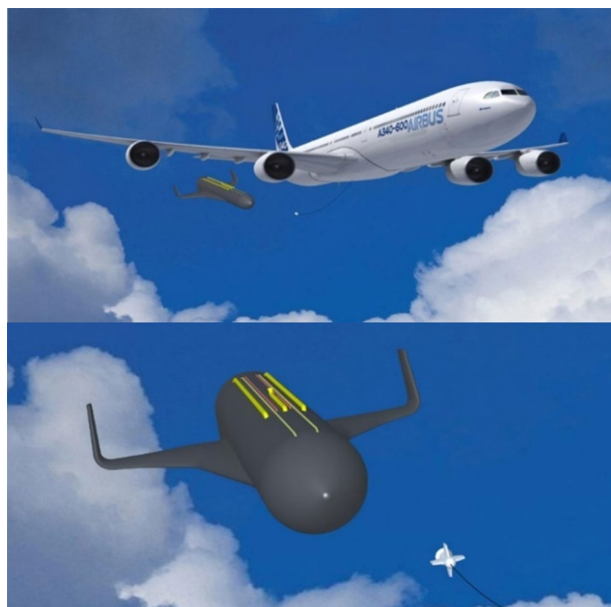

Fig. 1 Artist's impression of the IAC maneuver with the towing aircraft, capturing device and RLV stage (top) and the capturing device and RLV stage zoomed in (bottom)
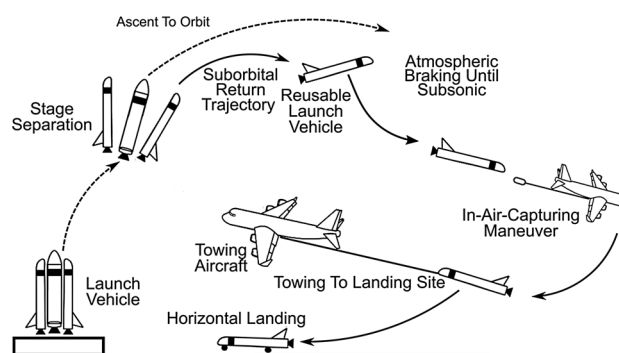

Fig. 2 Schematic of a typical IAC mission profile

flight parameters, while also providing sufficient thrust and range capability for the towed flight to the landing site. The ACCD has to ensure the mechanical connection to the RLV stage, while offering high agility to account for deviations in the position or any other disturbances. Furthermore, communication between the RLV stage, the TA and ACCD is crucial. Finally, the whole procedure should allow for multiple attempts and hence an extended time period to secure the connection. A detailed description of the vehicles and some important subsystems is given in Sect. 4.

The IAC process can be divided into five different phases:

- Formation flight: The towing aircraft matches velocity, position and heading to the RLV to establish a relative distance of 150 m–350 m.
- Capture phase: The ACCD corrects minor deviations between the vehicles and establishes mechanical connection to the RLV, while the TA and RLV remain in formation.
- Pull-up maneuver: Once connected, the aircraft (now connected to the RLV) increases thrust, followed by a climb to return to cruise altitude and velocity.
- Tow-back phase: It is the cruise flight to the landing site with the RLV being towed.
- Release Phase: RLV is released close to runway to autonomously land on the runway.

Of these phases, focus within this paper is put onto the first three phases, as they are the most critical for a successful IAC maneuver and are the ones least understood and simulated yet. The tow-back is mainly a form of typical cruise flight at more or less constant altitude and speed, while autonomous landing of winged stages is a challenge that was already demonstrated successfully in the past (Buran stage or Phoenix demonstrator).

2.1 FALCon project

The Horizon 2020-funded project, FALCon, started in March 2019 and ended in November 2022. The key goal was to increase the TRL of the IAC maneuver to 4–5 by focusing on three main areas:

- Development roadmap and economic benefit assessment.
- Experimental, subscale flight demonstration with UASs.
- Full-scale simulation and design.

The partners involved range from commercial to academic institutions and include DLR, VKI, Drone Rescue Systems GmbH, Soft2Tec GmbH, Astos Solutions SRL, the Institute of Mechanics of the Bulgarian Academy of Sciences and Embention. Within FALCon, actual flight hardware was developed and theoretic studies, in-depth analysis

and simulations of the full-scale scenario were performed. In this paper, a brief summary of the main results from the FALCon project are presented.

2.2 Recovery methods comparison

DLR has studied and compared different return methods extensively in the past [1, 3]. The considered return methods are vertical landing methods from SpaceX, either with downrange landing (DRL) or return-to-launch-site (RTLS) versus winged recovery methods like IAC or flyback (FB). Various metrics were used to compare the methods to each other such as mass, performance, re-entry loads and furthermore [1, 3]. One indicator that takes performance directly into account is the so-called inert mass ratio (IMR) as defined in Eq. (1). Here, the inert mass m_{inert} is defined as the mass of the vehicle at re-entry including dry mass, recovery hardware and additional required propellant. Dividing this value by the gross lift-off mass (GLOM) of the stage gives the inert mass ratio, which is directly linked to the Tsiolkovsky's rocket equation. A higher inert mass ratio indicates lower performance Fig. 3.

$$IMR = \frac{m_{inert}}{m_{GLOW, stage}} = \frac{m_{prop, remains} + m_{dry}}{m_{GLOW, stage}}. \quad (1)$$

Figure 4 shows this inert mass ratio for different return methods and propellant combinations versus each RLV stage's propellant mass. All vehicles are designed for the same payload of 7.5 t to GTO (details in [1, 3]). Since a high inert mass ratio indicates low performance and fewer propellant indicates lower GLOM and higher efficiency, the lower left region of the plot represents better options, while the upper right region represents worse design choices. One can clearly see that for hydrogen and hydrocarbons, the best option is IAC, offering both low inert mass ratio and low propellant mass. Although winged returning stages generally require more additional hardware such as wings,
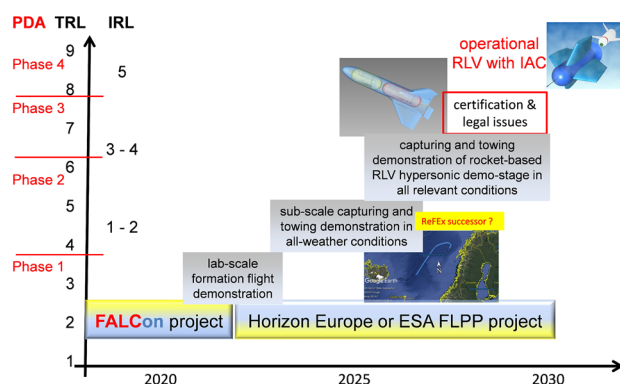

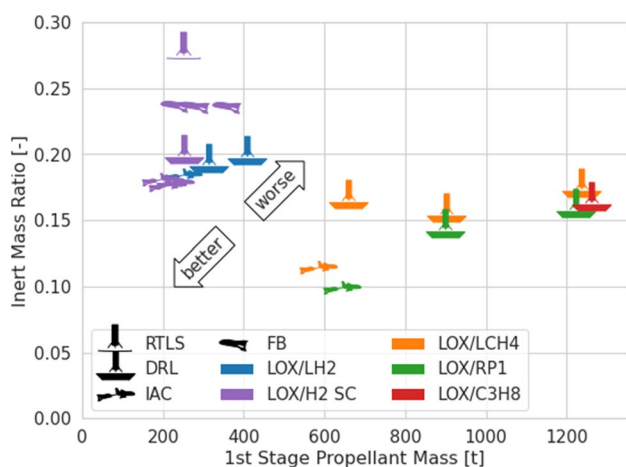**Fig. 3** Development roadmap for major IAC system demonstration

Fig. 4 Inert mass ratio versus propellant mass for different RLV types and propellant combinations

Fig. 5 RLV demonstrator (RLVD) during taxi testing [7]

aerodynamic surfaces and landing gear compared to vertical take-off vertical landing (VTVL) stages, this drawback is outweighed by eliminating the need for any return propellant. Furthermore, IAC also is better in terms of payload performance than FB methods, thus showing the general applicability and advantages this innovative method can offer.

Preliminary investigations of the costs linked to the recovery of the RLV stages have shown, that vertical take-off horizontal landing (VTHL) with IAC and VTVL methods generally end up at similar costs [8]. Nevertheless, the most important driver for the development of new launch vehicles remains the final launch costs. Here, it is difficult to obtain reliable cost data, since the methods used predominantly in launcher cost estimation (e.g., Transcost) are lacking data on RLVs [8]. Hence, establishing a more detailed cost model is important and foreseen for future work.

2.3 Roadmap

Within the FALCon project, a development roadmap was defined in cooperation with potential partners and European space stakeholders [5]. The currently envisioned roadmap to reach an operational RLV in the 2030 + years is presented in Fig. 3. After the laboratory-scale demonstration in FAL-Con with the current UASs, another subscale demonstrator would be needed for increased scale, increased speed, and capturing and towing in all relevant weather conditions and during day- and nighttime. Operational, certification and legal issues are to be addressed in the second half of the decade when a consolidated scenario has been established. Further possibilities could include testing the IAC method by using stages of micro-launchers as testbeds or capturing other kinds of re-entry configurations. However, the funding for this development roadmap is not secured beyond the

FALCon project as for now. More details about the development roadmap are presented in [5].

3 Flight testing with UAS

The subscale flight testing with UASs was one of the key objectives of the FALCon project, complemented by the simulation and analysis of the full-scale scenario. The flight-testing activities within FALCon include:

- Development, production and operation of reusable launch vehicle demonstrator (RLVD) and towing aircraft demonstrator (TAD).
- Development and production of subscale ACCD.
- Development of navigation system to aid the capture of the RLVD using the subscale capturing device.
- Simulation of subscale UAS in-air capturing scenario.
- Application for flight permissions, planning and execution of flight tests.

3.1 Unmanned aircraft demonstrators

To test the UASs representative of the full-scale scenario, a dedicated unmanned aircraft (UA) representing the RLV was developed by Embention within the FALCon project. This demonstrator is shown in Fig. 5. The geometry is based on a Rapier-Jet setup and has a length of 4.4 m with a wingspan of 2.6 m. To be representative of the full-scale scenario, the lift-to-drag (L/D) ratio can be reduced down to a value between 6 and 7. This low value is achieved by additionally deploying the landing gear during formation flight. The CoG is positioned at 70% of the vehicle's length, which is typical for RLV stages. The maximum take-off weight (MTOW) is 75 kg and the vehicle is propelled by a jet engine with a maximum thrust of 390 N. The jet engine is turned off for the IAC formation flight maneuver to represent the returning unpropelled RLV stage (Fig. 6).

Fig. 6 Towing aircraft demonstrator APUS [5]

The RLVD is equipped with a nose section, which houses the sensors for relative navigation. Those are camera and a LiDAR system for the close-range navigation between RLVD and ACCD. The camera detects light in the near-infrared spectrum which is emitted by LEDs positioned on the ACCD's capturing cone (see Fig. 7). The LiDAR system is able to estimate the ACCD's position relative to the RLV. The mission planning and flight control is processed by a 1X Veronte autopilot designed by Embention. For flight safety reasons, the RLVD is equipped with a rescue parachute [6].

As TAD, the APUS flight vehicle, which is operated by DLR, is used (see Fig. 6). This demonstrator has a length of roughly 3 m and a wingspan of 3 m. Its MTOW is 38 kg and as propulsion system a two-cylinder combustion engine is used. This engine is powerful enough to accelerate the demonstrator to its maximum velocity of 200 km/h. This demonstrator pulls the ACCD, which is attached via rope to its fuselage. As flight control system, a redundant setup with two Pixhawk Cube Orange autopilots is used. This allows beyond visual line-of-sight (BVLOS) mission planning for the UA formation flights. Similar to the RLVD, APUS is also equipped with a parachute system.

The ACCD used for the UA formation flight testing is shown in Fig. 7. The drogue contains LEDs emitting near-infrared light for the optical sensors, while the main body contains the flight avionics and aerodynamic control surfa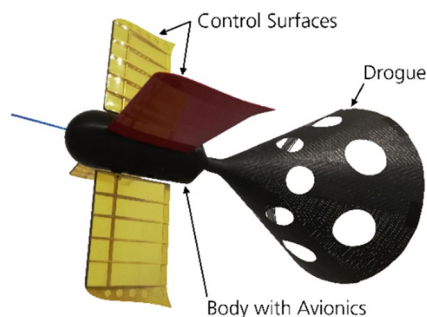ces. The capturing device is equipped with a redundant set of two Pixhawk 4 Orange autopilots, which allows control in the lateral and vertical directions behind the aircraft. For longitudinal corrections, the towing aircraft is equipped with a winch that can be used to shorten or lengthen the rope length.

3.2 Flight testing

The flight-testing location was chosen to be the National Experimental Test Center for Unmanned Aircraft Systems in Cochstedt, Germany. This test site for UASs is operated by DLR and is based on the site of a former commercial airport. For flight testing, the approval or necessary certification was provided for both the UASs by the German Federal Aeronautic Authority (LBA). Both the vehicles successfully acquired permits to fly BVLOS. The flight was allowed over sparsely populated area limited by a maximum height. Both vehicles, TAD and RLVD, were first flown individually. The subscale capturing device was also tested on the ground by towing it via a car.

The main goal of the flight testing is the demonstration of the formation flight between RLVD and TAD with establishment of physical contact between the RLVD's nose boom and the capturing device drogue. The schematic of the planned mission is shown in Fig. 8. The formation flight is planned to be established between an altitude of 655 m to 100 m above ground at a velocity of roughly 41.5 m/s. The FPA for the RLVD in gliding conditions is set to -10° with the option to test other glide path angles in later tests. The TAD is to fly in front of the RLVD and the capturing device will be released by the winch while using its aerodynamic control surfaces to establish mechanical contact.

The RLVD initially gains altitude and flies the red path shown in Fig. 8. Once it reaches the approach point (AP), it turns around and prepares to begin the IAC maneuver. For synchronization of the trajectories, the last circular radius of the TAD is adapted based on its current position in the circuit when the RLVD reaches AP. The TAD
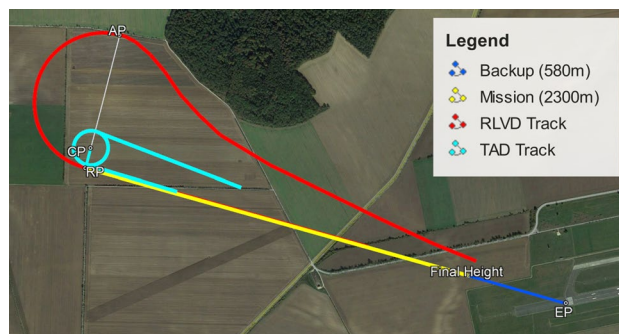

Fig. 7 Subscale capturing device for demonstration

Fig. 8 Planned mission trajectory for demonstration of IAC using laboratory-scale vehicles

follows the blue path and loiters in circles until the RLVD starts the approach. The rendezvous point (RP) marks the beginning of the mission and the end point (EP) marks the end of the mission. Once both vehicles are in vicinity at the rendezvous point (RP), the formation flight is attempted along the yellow path. The formation flight is divided into two main parts: first, a rough formation flight based on GNSS navigation where the RLVD communicates its position and velocity to the TAD, which positions itself in front of the RLVD. Once this rough formation is established and the RLVD is within 20 m of the TAD, the close-range navigation system based on an IR camera and LiDAR is then used to allow position estimates with much higher accuracy [6]. Next, the capture of the RLVD is attempted by the subscale capturing device until a connection is established (while both vehicles remain in formation).

During the final test campaign of the FALCon project held in September 2022, an unfortunate anomaly in the rescue system led to the premature deployment of the parachute of the TAD. Due to the low-altitude deployment, the parachute failed to deploy correctly and the motor power was cut off by the rescue system. Due to loss of steering capability, a controlled impact was conducted to avoid complete loss of the UA. This led to damages to the TAD that could not be repaired before the end of the project.

Although the final integrated IAC demonstration could not be completed within FALCon, the individual flight tests yielded valuable flight data. Important subsystems like the autopilot, companion computer and avionics were tested during the individual RLVD flight. Similarly, TAD hardware and controller was also tested in flight. The subscale ACCD was tested in wind tunnels and gained insights on further development of a smart drogue with active control surfaces. Static ground tests were also performed, where ACCD was towed by a car and allowed to fly freely. This played an important role in testing of sensors, controller as well as the winch mechanism that controls rope length. This data was used for realistic simulations of the subscale IAC maneuver and will be presented in Sec. 5. Hence, the UAS flight testing was investigated and simulated in theory and still marked a major milestone for the FALCon project.

4 Full-scale vehicle design

As explained earlier, the IAC recovery method requires the RLV stage to be actively captured by a TA with an ACCD in flight. The design considerations with regard to each of those vehicles are presented in this section.

4.1 RLV stage

In the framework of RLV studies at DLR, several multi-mission vehicles consisting of two to three stages, serving a maximum payload mass of 14 t to GTO, were studied [9, 10]. The RLV first stage of the LOX-LH2 system propelled with staged combustion engine was used as reference stage for FALCon (see Fig. 9). The RLV stage has to fulfill a range of important requirements for a successful IAC. First, during re-entry, the stage has to be controllable throughout a vast range of flight conditions. Typically, the re-entry initially starts with a high angle of attack (AoA) and high velocity and the AoA is gradually reduced during the deceleration phase. At subsonic velocity, however, the L/D ratio should be as high as possible to allow for flight with a shallow FPA. This facilitates the matching of velocity and FPA by the TA. For RLV stages, an L/D ratio at subsonic velocity above 6 is aimed for. Therefore, a foldable outer wing, which is deployed at subsonic velocities, is considered to achieve a high L/D ratio.

The RLV stage used in FALCon has a total dry mass of 71 tons and a total length of around 56 m with a diameter of 5.4 m [9, 10]. The outer wings when deployed, as shown in Fig. 9, have a wingspan of 35.5 m. The aerodynamic control in pitching axis is achieved by a body flap at supersonic velocity plus elevons at the inner trailing edge of the double-delta wings. For lateral control, the trailing edge flaps of the
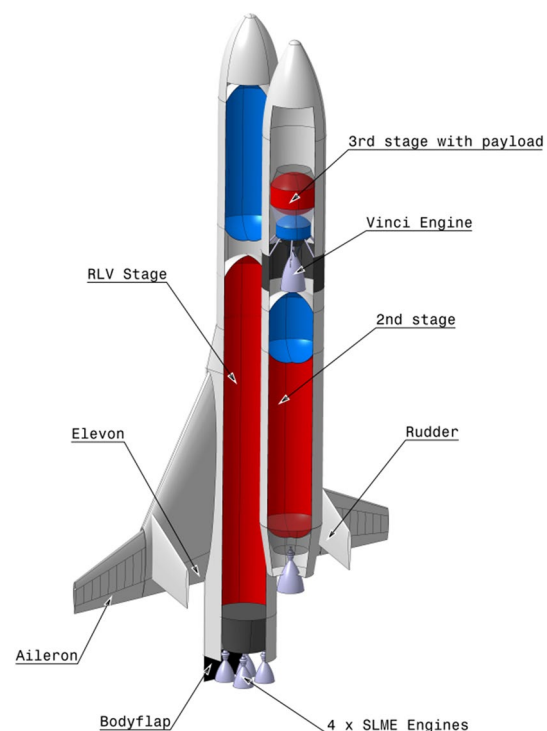

Fig. 9 Reference RLV launcher concept with three stages

outer wing are used as ailerons and two rudders are installed on the wing.

In the design process, the aerodynamic properties of the stage were first calculated using empirical in-house methods (based on DATCOM). The L/D ratio for trimmed flight from this analysis is shown in Fig. 10. The L/D ratio at Mach 2 and beyond is at a maximum of 2 at around 10°, which is typical for such winged re-entry vehicles. The maximum subsonic L/D is around 6, which should be sufficient for the IAC formation flight maneuver (Figs. 11 and 12).

Within the FALCon project, CFD analyses of the flight point most probable for IAC at subsonic velocity were performed to cross-check the aerodynamic data [11]. The respective L/D ratios for this flight point with a velocity of Mach 0.45 at an altitude of 6500 m are shown in Fig. 13. The CFD data produces a slightly steeper slope with an even slightly higher maximum L/D ratio of 6.1 at an AoA of around 10°. The respective data was used for the full-scale simulations of IAC as shown in Sect. 5.

The re-entry trajectory of the RLV stage following its separation from the rest of the launch vehicle is shown in Fig. 11. The vehicle is controlled via reaction control system during exo-atmospheric flight and via the aerodynamic control surfaces once the atmosphere gets denser. The main deceleration of the vehicle takes place between 20 km and 50 km altitude with an initially high AoA to provide high lift and drag. Then, the AoA is gradually reduced in order to limit the maximum heat and structural loads onto the stage.

The IAC would commence at the end of the trajectory shown in Fig. 11. The stage enters a condition of rather steady gliding flight with a flight path angle of around −10° and a velocity of around 200 m/s at an altitude of 10 km. From here on, a different guidance would be initiated that aims for a rather shallow FPA without saturating
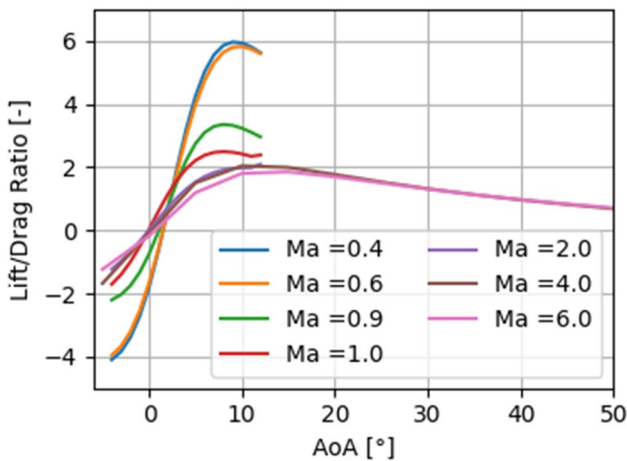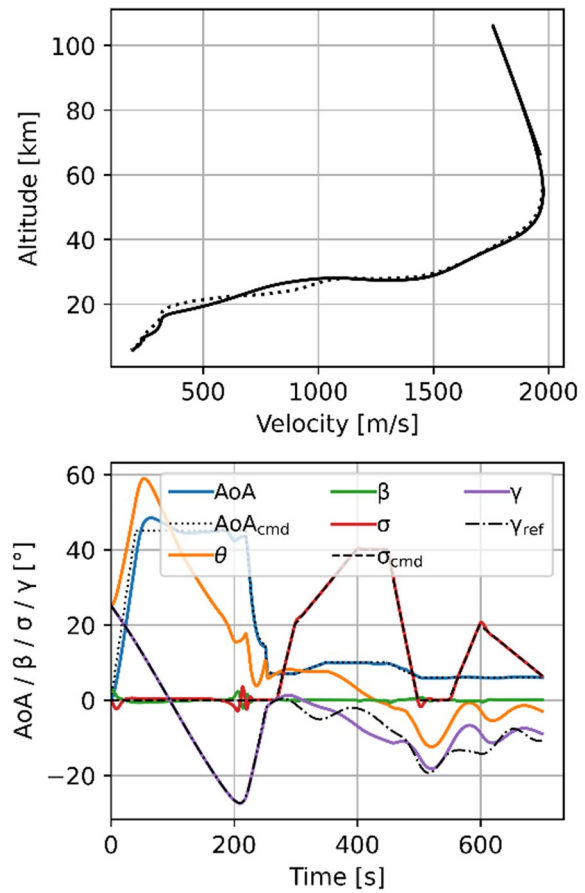

Fig. 11 Re-entry trajectory of the RLV reference stage in 3DOF (dotted) and 6DOF (solid) [10]

the aerodynamic controls. Those simulations are shown in Sec 5. Details about the trajectory simulation are presented in [10].

Fig. 10 L/D ratio for the RLV stage as calculated with empirical methods

Fig. 12 The A340-600 in clean configuration (top) and in IAC configuration (bottom) [11]
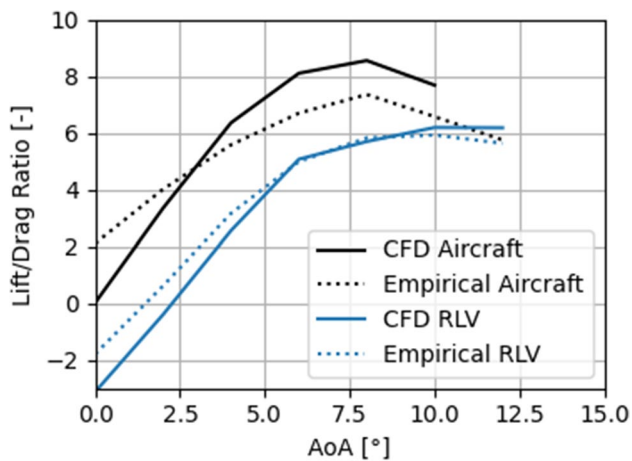
Fig. 13 L/D ratio of the RLV stage and the TA calculated with empirical methods and CFD simulations

4.2 Towing aircraft

Within FALCon, an A340-600 is selected as the TA for the capture of the large RLV. These can be acquired on the secondhand market for reasonable prices [8]. The A340-600 is propelled by 4 Rolls Royce Trent 556 engines, which renders it powerful enough to conduct the IAC maneuver and tow the RLV stage to its landing destination. Nevertheless, the A340-600 has a much higher L/D ratio than the RLV stage, which would make it difficult to achieve a similar gliding FPA, even with engines turned off. Hence, to decrease lift and increase drag, some measures have to be taken.

During the formation flight procedure, the aircraft deflects its spoilers on the upper wing surface by about 20°. Further, the landing gear (front and under the wings) is extracted completely, thus significantly increasing the drag as shown in Fig. 12. The engines are kept in idle mode (minimum throttle setting). A further design change would be to remove the center landing gear to accommodate the ACCD and the attachment of the rope to the aircraft. A more detailed breakdown of the design changes to the aircraft is given in [13]. These design changes lead to a vast reduction in L/D. The respective values, calculated per CFD analyses, are shown in Fig. 13 [11]. The agreement with the empirical data is moderate, since the aerodynamic configuration with landing gear and spoilers extended is difficult to assess via empirical methods. Nevertheless, the maximum L/D ratio of the TA is 8.5 according to CFD simulations, which is rather close to the maximum L/D ratio of the RLV. Section 5 shows in detail the simulations of the formation flight maneuver using the CFD aerodynamic data.

4.2.1 Wake field behind towing aircraft

The formation flight during the IAC maneuver involves close proximity of the RLV to the aircraft. The wake field of the TA, especially when the engines are running, will produce disturbances and, thus, have an impact on the ACCD and RLV flying in its wake field. Therefore, a characterization of the wake field was performed to evaluate this impact and take it into account in the 6DOF full-scale analysis.

RANS simulations were performed with the IAC configuration of the aircraft at 0° and 6° AoA. A detailed overview of the numerical methodology used for RANS simulations are provided in [11, 12]. The respective flow field is shown in Fig. 14 and the velocity components in the flow field are shown in Fig. 15. Those components are expressed with respect to a free stream velocity of $u_\infty = 142$ m/s. It can be observed that the aircraft produces a significant downwash (vertical) component, leading to a velocity component of almost 10% of the freestream velocity, so about 14 m/s. Even in a distance of almost 315 m to the nose of the aircraft, the downwash component is at 8% of freestream velocity. This downwash component alters the AoAs of the vehicles flying in the wake. Thus, it could lead to quite some disturbances for any vehicle crossing the wake field (Fig. 13).

4.3 ACCD

The ACCD is the device that is attached to the end of the rope, which in turn is connected to the towing aircraft. It serves as the device establishing the mechanical connection between the RLV and the aircraft during formation flight. Therefore, it needs to be aerodynamically controllable to account for disturbances and deviations of the RLV. Also, it needs to communicate with the RLV to know its position and correct errors. The communication methods used can be adapted from the current subscale scenario [7]. However, adaptations would have to be necessary to fit the

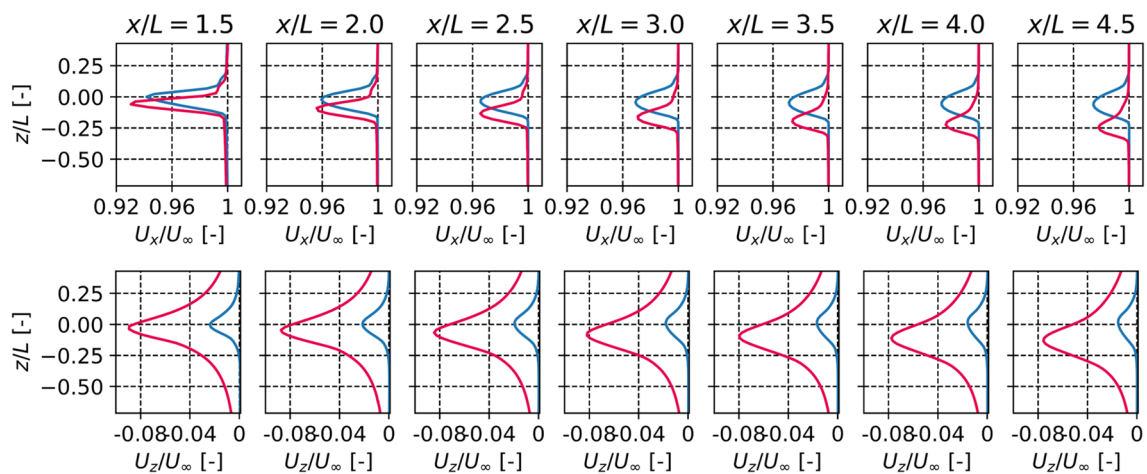**Fig. 14** Flow field behind the towing aircraft for 6° AoA [11]
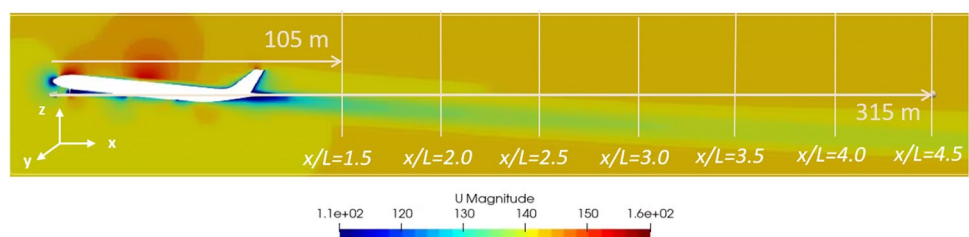
Fig. 15 Velocity Components in the wake field at an angle of attack of 0°(blue) and 6°(red): streamwise velocity component UX (top) and downwash velocity UZ (bottom) with reference to a freestream velocity of U∞ [11]

communication hardware to the full-scale scenario. Further avionic systems, like an onboard computer, GNC systems and, optionally, a battery would be placed inside the ACCDs rigid body.

Figure 16 shows the reference ACCD for the full-scale IAC scenario within FALCon. Its total length is 2 m and its wingspan 1.5 m. The vehicle is axisymmetric with four symmetric fins that are equipped with movable flaps at their rear part. Thus, the vehicle can be controlled in roll, pitch and yaw independently. The ACCD weighs about 165 kg.

The aerodynamic database was built by extensive CFD RANS simulations [11]. The aerodynamic force and moment coefficients for each axis were calculated for different fin deflections and varied AoAs. Thus, a complete CFD-based database was established that uses a linear superposition procedure to calculate the aerodynamic coefficients at any flight point [14]. Due to the use of RANS methods, effects like fin shadowing or stall are considered in the aerodynamic database.

4.4 Rope

The final element in the IAC maneuver is the rope connecting the ACCD to the aircraft. It has to be strong enough for capturing and towing of the RLV stage, while having a minimum mass to not hinder the maneuverability of ACCD. For this purpose, a rope made of the material UHMWPE (ultrahigh molecular weight polyethylene) was chosen since it offers high strength and low density, leading to a light-weight rope. The material is widely used in marine, sports, medical and space applications. The length of the rope is determined by the outcome of the 6DOF simulations and depends on factors such as controllability of the ACCD, towing flight dynamic performance and mass of the rope.
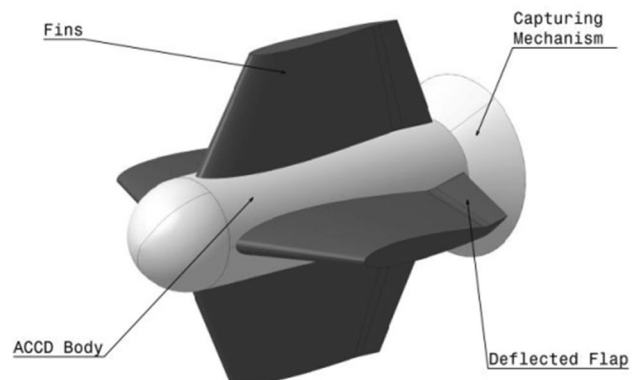

Fig. 16 ACCD with four fins and capturing mechanism

Completely deployed, a rope length of 150 m–350 m is the range considered in FALCon. The diameter of the rope also has a major impact on the dynamics of the whole IAC procedure. Different diameters were subjected to an analysis and a diameter of 16 mm was selected for now [15, 16]. The mass of a 16 mm rope with a length of 150 m is 23.4 kg.

The rope can be released by a winch mechanism, which is installed at the attachment point of the rope to the aircraft, presumably the middle landing gear bay (refer to Sec 4.2). Currently, it is undecided if the power supply of the ACCD will be autonomous onboard supply via a battery or if an electrical cord will run along the towing rope.

Within the full simulation of the IAC maneuver, the rope is simulated as depicted in Fig. 17. It is composed of several discrete elements, which are connected by springer–damper elements to model the flexibility of the rope as shown in the figure. The bending stiffness is modeled by identical springs with a non-linear stiffness at each element. The aerodynamics are included by introducing a drag model. Further details about the rope modeling can be found in [13]. The ACCD's
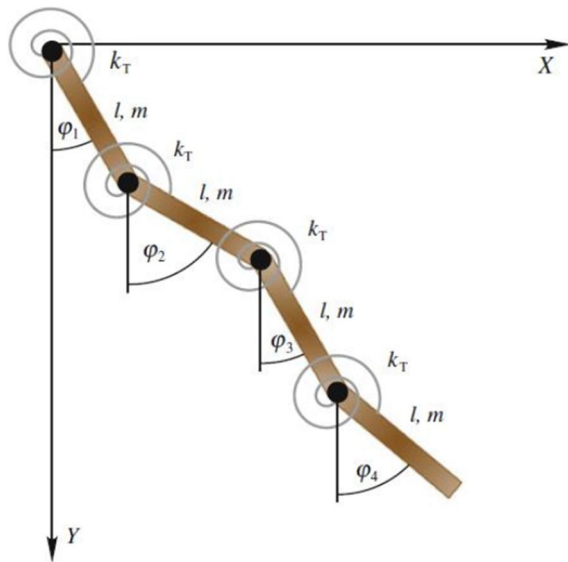
Fig. 17 Discretized rope model used for IAC simulations

attachment is modeled by an almost rigid connection to the rope with a very high damping coefficient. This has shown to stabilize the whole system of rope and ACCD dynamics in the wake field of the aircraft.

As the outcome of the simulations also depend on numerical factors such as discretization of the rope, number of elements, diameter and length, a range of sensitivity analyses were performed to narrow down the design space for the rope. This sensitivity analysis showed that a discretization into 30 elements is sufficient for this task [16].

5 Simulation of the IAC maneuver

In this section, trajectory simulations are presented for both subscale and full-scale scenarios. The different flight phases are for now simulated separately, since a connected and complete simulation will be subject to future work. However, understanding the challenges and characteristics of every phase of the IAC maneuver itself is already a major step toward maturing this technology. First, the preliminary full-scale simulation results are presented. The formation flight, capture phase and the pull-up maneuver of the IAC procedure are evaluated. Then, the subscale simulations using flight data are presented for the formation flight and capture phase. The results are compared and evaluated for both the scales and the future steps are proposed accordingly.

5.1 Full-scale trajectory simulations

Preceding the formation flight, the RLV stage re-enters the atmosphere mainly aerodynamically controlled, and

gradually slows down to subsonic velocity. At approximately 10 km altitude, the IAC process begins. Considering the full-scale test cases selected in FALCon, trajectory simulations are performed and presented as follows.

5.1.1 Formation flight

Once the RLV stage enters a state of gliding with a constant FPA, the aircraft will transition from its loitering flight state to a diving flight, where it will match the RLV stage's velocity and heading, and positions itself in front of the RLV. The ACCD can be released during this dive or prior to it. Releasing the ACCD prior to the diving flight would allow for checkups of system functionality with sufficient time ahead of the actual IAC maneuver.

Once the aircraft enters the formation flight in IAC configuration, landing gears and spoiler are deployed for extra drag. The requirements for the formation flight were defined as follows [17]:

- The formation flight should be achieved within an altitude of 8000 m to 3000 m.
- The relative distance between RLV and aircraft should be between 70 and 350 m.
- The relative altitude should not exceed ± 150 m.
- The relative velocity between the aircraft and the RLV should not exceed ± 3.5 m/s.
- The control surfaces should be unsaturated to allow for maneuverability.

The simulations were performed in 3DOF with actively controlled RLV and TA. The RLV here follows a 3DOF trajectory with the maximum possible descent FPA ($-8°$), while the aircraft tries to match speed and FPA. Figure 18 shows the results of this analysis. The green area marks the region where the requirements of the formation flight are met. This area stretches over a time period of close to 70 s. A detailed explanation of the study is presented in [17].

The plots show that the aircraft can match the RLVs velocity sufficiently close, but the FPA is higher, leading to a shallower gliding flight of the TA. This means that the RLV stage is not at a constant vertical distance to the aircraft, but is descending from the aircraft's point of view. This gap would have to be compensated by the ACCD. The effect of wake can be observed as a disturbance is the FPA of the RLV as it gets closer to the aircraft. Nevertheless, the formation flight could be achieved with wake disturbances.

As a further measure, it was investigated what effect turning off the engines would have on the trajectory. As expected, the formation flight duration can be increased and the FPA can be matched closer to the FPA of the RLV. This would allow formation flight of more than 60 s in some cases, as was investigated by a sensitivity analysis
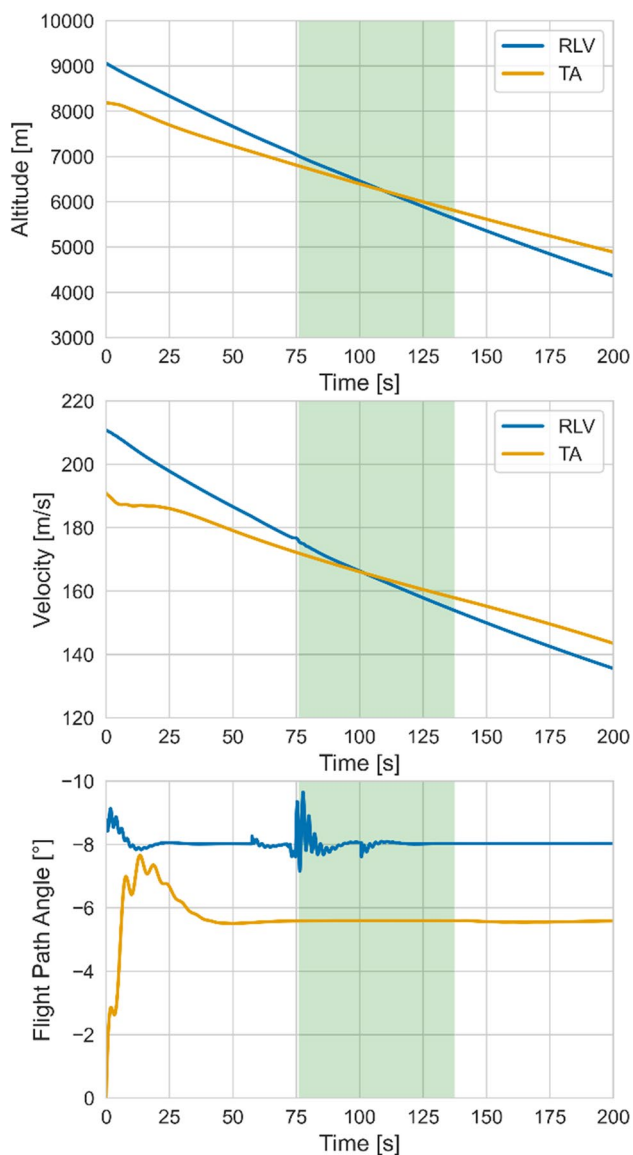
Fig. 18 Formation flight trajectory with no idle thrust and wake disturbances included

of the aircraft's initial conditions onto the formation flight duration [13, 15]. Nevertheless, turning off all engines in flight is a critical maneuver that would need further discussion with experts, as it takes away flexibility in controlling speed and altitude in case of non-nominal behavior. Furthermore, the power provided by the engines is lost, so the aircraft has to rely on the power provided by the auxiliary power unit (APU).

Another means of prolonging the formation flight would be to somehow increase the drag of the aircraft. A possibility to do that would be to induce an angle of sideslip by engaging the aircraft's rudder and ailerons. This increases the drag and the descent rate, leading to a steeper descent

of the aircraft. This maneuver was not yet investigated, but will be considered in future work.

5.1.2 Capture phase

The capture phase is defined as the phase where the ACCD's active maneuvering establishes mechanical contact between ACCD and RLV during formation flight. The capture phase is modeled and simulated in 6DOF, with actively controlled ACCD, the rope and TA model included. The ACCD's controller was designed to control the vehicle to a commanded position in the vertical and lateral axis (so movements up and down, and left and right with respect to the aircraft). The controller tuning was performed at steady flight conditions without the wake field of the aircraft and basically consists of PID control of the inner loop, commanding roll, pitch and yaw, and a PID controller for position in the outer loop. Details about this controller are presented in [13] and [16].

The results for two different scenarios are presented: one where the ACCD is positioned at a stable point behind the aircraft and is commanded certain movements without the wake field's influence considered; and the other scenario essentially the same with the wake field included. The rope length in both cases is 150 m with a diameter of 16 mm. Figure 19 shows the trajectory of the ACCD with respect to the aircraft for commanded movements in the y and z-axis. The movement in x-direction is only a result of those movements combined and is not an actively commanded value. As can be seen in the plot, the ACCD is capable of following the commanded path sufficiently well even in the presence of the rope vibrations, which are eventually damp out [13, 15, 16]. Also, it is important to note that the aerodynamic control surfaces of the ACCD remain unsaturated to allow for further control margins.

In contrast, the respective simulation results for the wake field active are shown in Fig. 20. With the turbulence and the downwash active, the ACCD is not capable of following the commanded profile. When moving to the commanded z-position of 10 m, the wake intensity grows as do the oscillations of the ACCD. The controller, which was tuned for steady conditions, does not take into consideration the change in free stream velocity due to wake. In future, an advanced control design would be considered for effective operation of ACCD even with wake disturbances.

Another measure to help diminish the oscillations would be the use of a longer rope. A longer rope further would allow for greater movements of the ACCD while positioning the ACCD further lower compared to the aircraft's middle axis, thus positioning it away from the major turbulences in the wake field. Also, the intensity of turbulences decreases with distance to the aircraft as shown in Fig.14. Simulations of ACCD capturing the RLV are also to be performed in future.
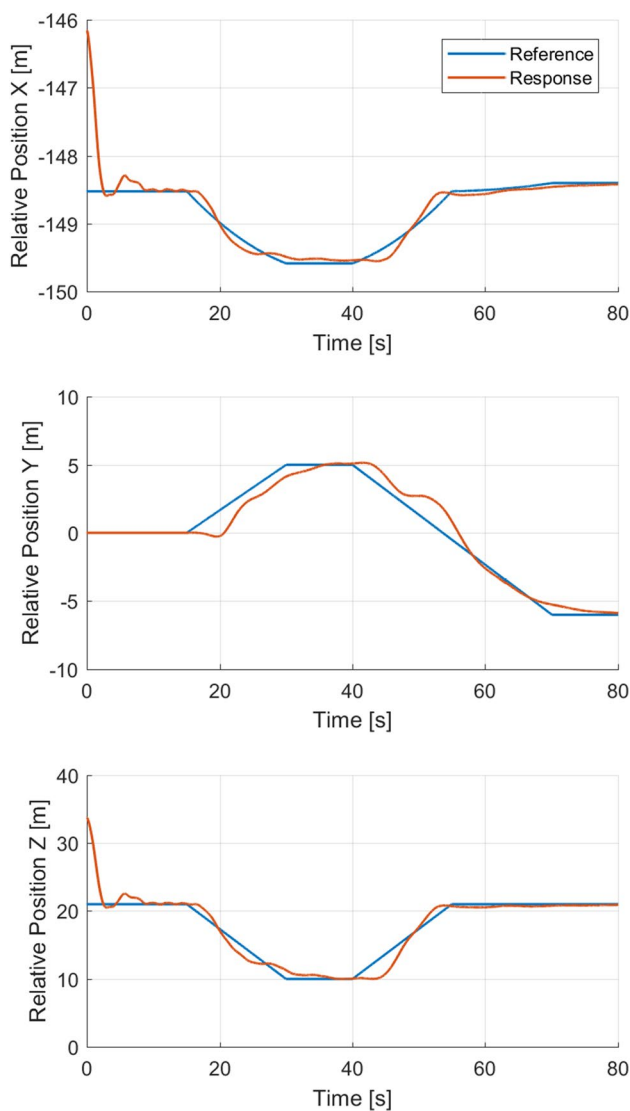
Fig. 19 ACCD response to controlled position without wake when the aircraft is in steady flight

5.1.3 Pull-up maneuver

The pull-up maneuver is initiated once successful capture of the RLV can be confirmed. The aircraft would then retract spoilers and landing gear, increase thrust and transition to a horizontal flight with the RLV being towed. Then the mated configuration would start to move to its designated cruising flight conditions.

The pull-up maneuver is divided into three different steps:

- Landing gear and spoiler retraction: aerodynamic database shifts from IAC to cruise flight configuration by linear transition (Step 0).
- Aircraft throttle up to 100% (Step 1).
- Climb or descent to cruise flight conditions (Step 2).
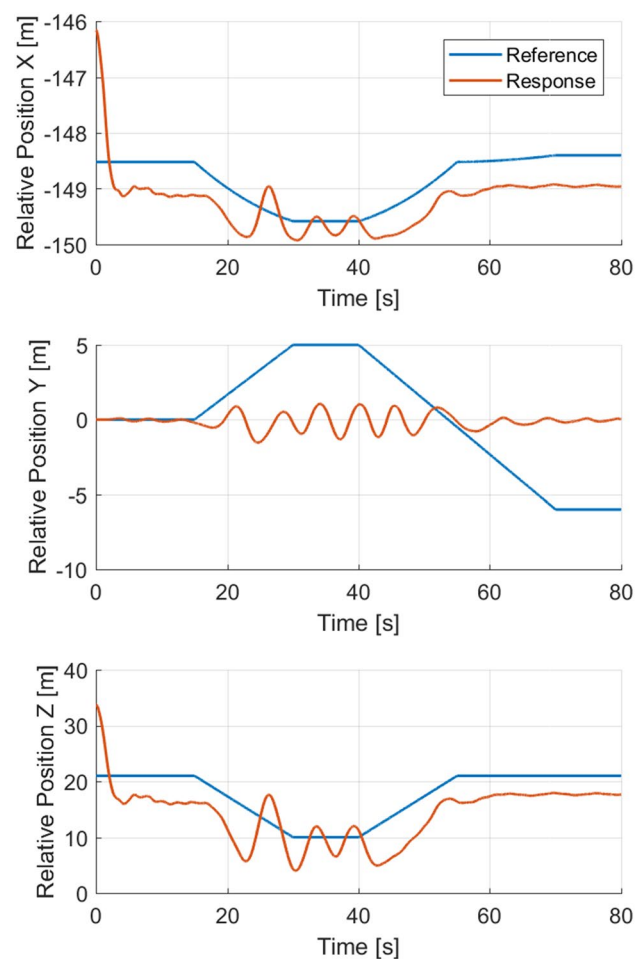
Fig. 20 ACCD response to controlled position with wake when the aircraft is in steady flight

- Cruise flight (Step 3).

The aircraft is controlled by a PI controller for altitude and a PID controller for velocity [18]. The RLV is controlled by a PID flight path angle controller and a PI altitude controller actively changing its pitch angle. In these preliminary simulations, the rope model is simplified as for now, assuming a rigid link between the aircraft and the RLV that constrains translational, but allows rotational, movement as shown in Fig. 21.

Figure 22 shows the results of the trajectory simulation when the wake of the aircraft is not considered. After the landing gear and spoilers are retracted, the aircraft increases its AoA to 13° to induce the pull-up maneuver. The RLV actively tries to match its FPA to the aircraft's FPA, which can be done in sufficient accordance [18]. However, the RLV's aerodynamic control surfaces, namely the elevons, get saturated at this point. Following the pull-up maneuver, the subsequent climbing and cruising flight can be maintained and cruising conditions are reached after around
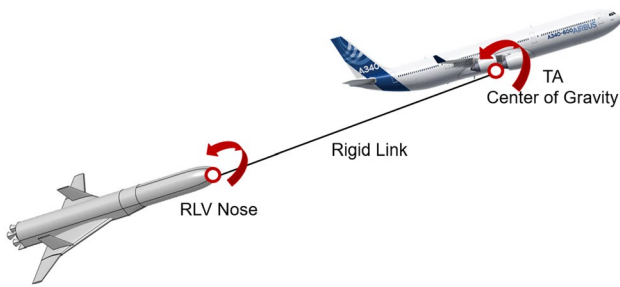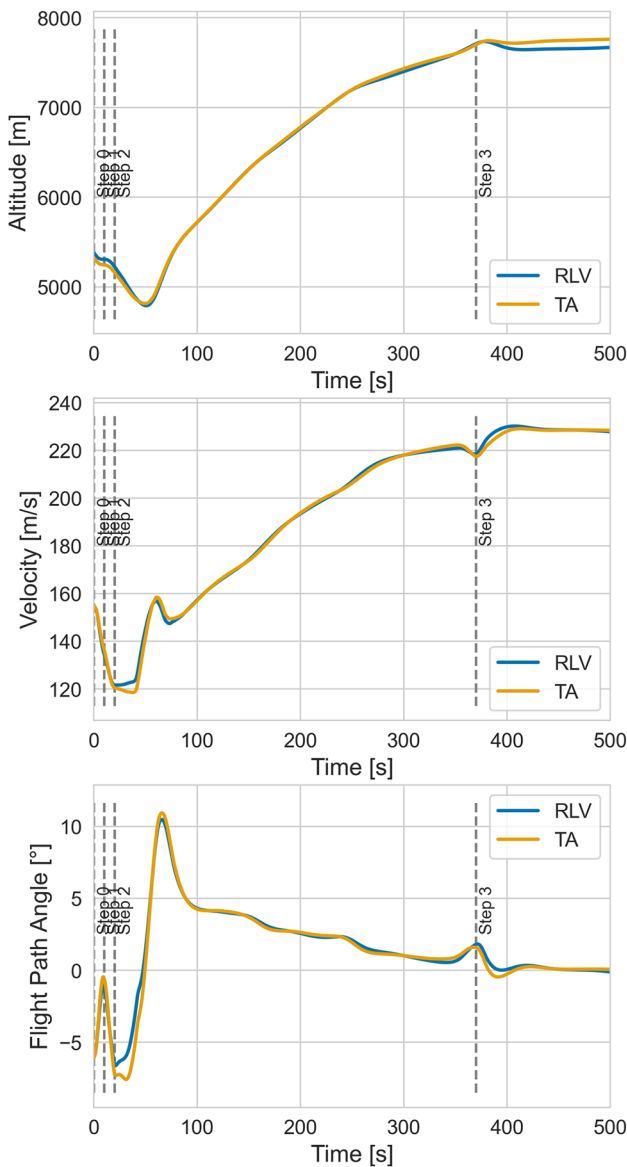
Fig. 21 Schematic of the pull-up maneuver

Fig. 22 Preliminary simulation of the pull-up maneuver

6 min following successful capture. The study also indicates that the thrust from the aircraft is sufficient to tow the RLV. For future work, the more detailed rope model from the formation flight simulations as well as the wake field should be included, leading to potentially more critical maneuvering during the pull-up.

5.2 Subscale trajectory simulations

The final demonstration of IAC maneuver could not be completed within FALCon. However, the demonstrators were tested and flown individually, which helped collect critical data for control tuning, sensor integration, further flight planning and simulations. The simulated trajectory shown in Fig. 23, attempts to replicate the originally planned mission trajectory (shown in Fig. 8). The RLVD trajectory (blue) is directly derived from the flight data of the flown trajectory in the individual flight tests. The TAD guidance is then adjusted and simulated to perform IAC maneuver with the flown RLVD trajectory. The 6DOF simulations also take into account the sensor fusion as defined in [7].

The RLVD starts the mission around AP, after which it turns around to attempt formation flight with the TAD. The TAD loiters in circles until the RLVD reaches the RP. At this point, both vehicles try to achieve a formation flight, with matching velocities and altitude in a descending flight. The ACCD is towed by the TAD during the flight and only becomes functional when the RLVD and TAD achieve a relative distance of 20 m. In Fig. 23, the red cross marked by 'Coupling' shows the point where the connection is established between the RLVD and the ACCD. Detailed analysis of the formation flight and capture phase are presented in the coming sections.

5.2.1 Formation flight

Identical to the originally planned flight tests, the formation flight in simulations must be established between an
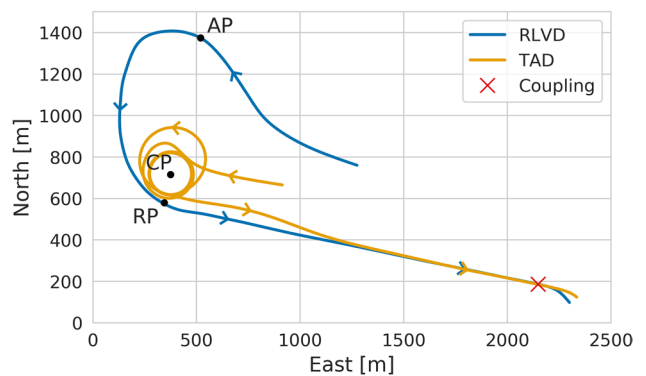

Fig. 23 Trajectory simulation of subscale IAC trajectory

altitude of 655 m–100 m aboveground at a velocity of roughly 41.5 m/s. For the subscale simulations, the wake from the TAD was not considered. Figure 24 shows the altitude, velocity and FPA of the simulated formation flight. The green shaded area again shows the region in which the formation flight is successfully achieved. Here, the relative distance between TAD and RLVD is smaller than 20 m and the velocity is also in close agreement.

It can be observed that approximately 20 s of formation was achieved. Compared to the full scale, the formation is maintained for a smaller duration. However, the duration was mainly limited by the space limitations of the airfield and the acquired flight certification. Future flight tests will
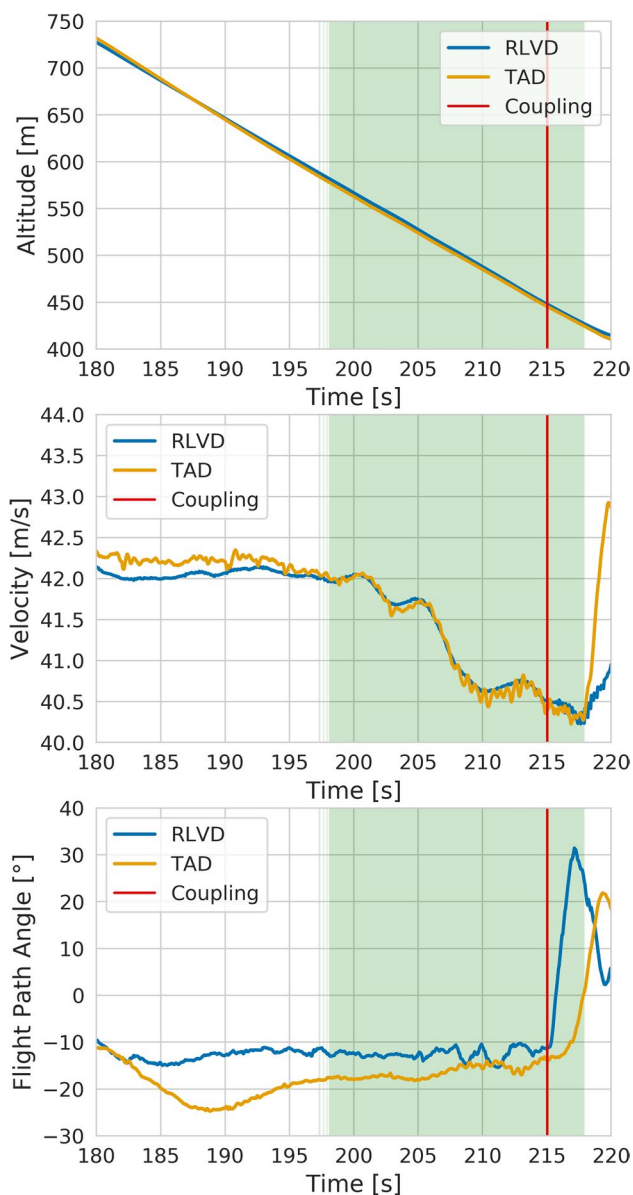
Fig. 24 Formation flight trajectory of subscale aircraft

aim to achieve longer formation durations with larger-scaled vehicles. The end goal is also demonstration of IAC in non-ideal weather conditions and poor visibility.

It can be observed that the RLVD trajectory data acquired from the flight test does not maintain constant velocity during the formation flight. This is mainly because of the disturbances originating from shutting off engines mid-flight, leading to loss of velocity while the autopilot attempted to keep a constant FPA. Wind gusts during the flight tests also contribute to some of the disturbances.

5.2.2 Capture phase

During the 20 s formation flight, the subscale ACCD tries to mechanically connect the TAD and the RLVD. The close-range navigation is used to determine the accurate relative position of the ACCD with respect to the RLVD boom.

Figure 25 shows the relative position of the ACCD in the X-, Y- and Z-directions, obtained from sensor fusion of LiDAR and IR camera. When the relative Y-position nears zero and the relative Z-position is within 2.5 m from the RLVD boom, the rope is further unwound to cover the remaining distance along the X-direction. This is achieved through a winch system housed inside the TAD. At 215 s, the coupling of the ACCD with the RLVD is successfully achieved.

From Fig. 24, it can be observed that the coupling is already achieved approximately 17 s into the formation flight. A longer formation flight could allow for multiple attempts on capture and will be examined in future. Further, the subscale experiments were only to be demonstrated until the point of capture of the RLVD (marked by 'coupling' in Figs. 24 and 25). The pull-up maneuver and other phases of IAC are also to be demonstrated in future (Fig. 25).

6 Conclusion

Within the framework of the FALCon project, an innovative recovery method for reusable rocket stages, the in-air capturing (IAC) method, was investigated thoroughly. By detailed simulation and analysis of the full-scale scenario, involving an RLV stage, a towing aircraft and an aerodynamically controlled capturing device (ACCD), the knowledge and understanding of this method was deepened. New insight about the challenges and characteristics of this recovery methods were gathered especially in the fields of aerodynamics, flight dynamics, simulation in 3DOF and 6DOF, definition of a full-scale system and development roadmap. These insights surely helped in increasing the technology readiness level (TRL) of this technology.

Considering the full-scale scenario, an RLV reference launch system was defined whose first stage was used as
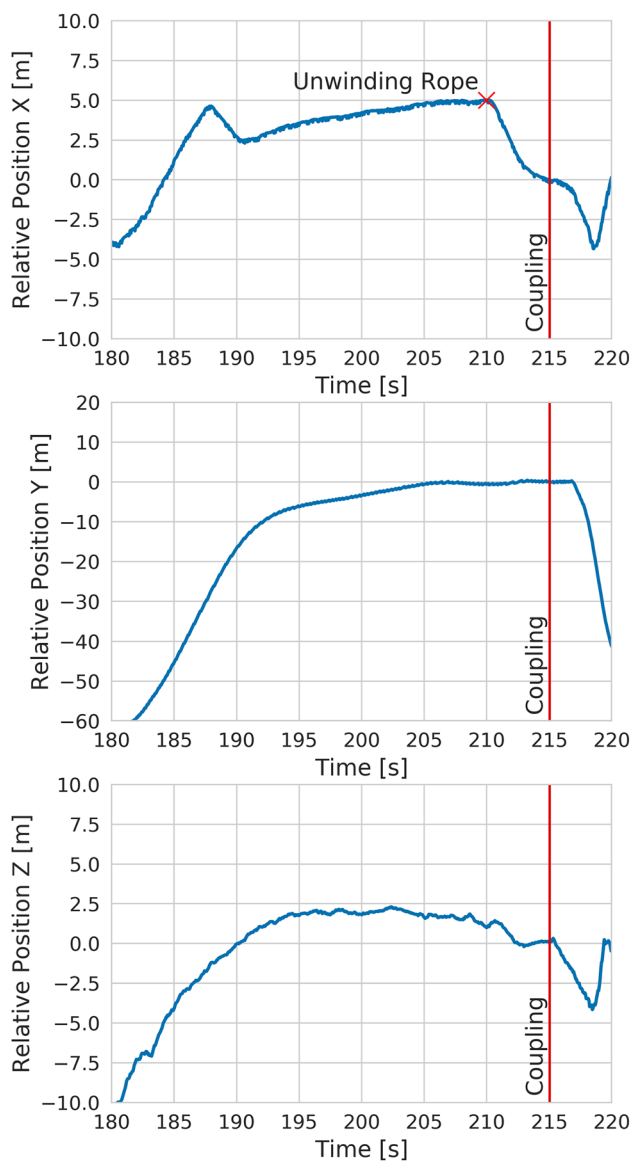
Fig. 25 Relative position of subscale ACCD to the subscale RLV during the capture phase

reference stage for the subsequent IAC simulations and analysis. Furthermore, a thorough study on aircrafts led to the selection of the A340-600 as reference aircraft, including an analysis of possible modifications. Furthermore, the aerodynamics of this aircraft and its wake field were characterized by CFD simulations. An aerodynamically controlled capturing device (ACCD) was defined and an aerodynamic database was built by CFD simulations [14, 16].

The aerodynamic models were subsequently used in the simulation of the IAC maneuver itself, divided into several phases. For the first time since the invention of the IAC method, 6DOF analysis of the trajectory could be performed including complex rope dynamics, wake

field interactions and vehicle dynamics. Thus, the general feasibility of this procedure could once again be proven. However, there is still room for improvements, especially considering formation flight duration. Here, increasing the drag by either allowing flight with an angle of sideslip or turning off some of the engines might improve the situation. This shall be investigated in future work.

During FALCon, multiple unmanned aircraft systems (UASs), within 100 kg class, were developed for the demonstration of IAC in subscale. The reusable launch vehicle demonstrator (RLVD), towing aircraft demonstrator (TAD) and the subscale capturing device were first tested individually in flight and on ground. The final integrated flight testing, attempted in the fall of 2022, was performed to demonstrate the complete IAC maneuver. The goal was to demonstrate the formation flight between RLVD and TAD, wherein the vehicles fly close to each other in a descending flight and with similar velocities. During this, a physical contact was to be established between the RLVD's nose boom and the capturing device. However, due to an anomaly during the flight tests, the TAD demonstrator suffered significant damage, which could not be repaired before the end of the project.

Nonetheless, the development of UASs led to a gain in knowledge concerning vehicle design, flight controls, mission planning and environment perception. The process also provided some insight regarding the UAS development and licensing challenges that can be translated to the full-scale scenario. Flight data acquired from the individual flight tests also proved to be valuable in realistic simulation of the subscale IAC scenario. Furthermore, the common heritage of IAC with air-to-air refueling facilitates the future flight testing outside the scope of FALCon. Thus, the data acquired from upcoming flight tests (Summer 2023) for air-to-air refueling will be used for further development of IAC. The planned campaign by DLR would involve reuse of the same TAD and capturing device as that in FALCon.

In this context, the FALCon project can be already considered a success, rising the TRL of the IAC method to enable frequent, safe and reliable capturing of winged returning rocket stages by aircraft in the future.

Data availability Not applicable.

Declarations

Conflict of interest The authors declare that they have no conflict of interest.

References

1. Stappert, S., Wilken, J., Bussler, L., Sippel, M.: A systematic assessment and comparison of reusable first stage return options. In: Proceedings of the International Astronautical Congress, IAC. 70th International Astronautical Congress, Washington DC, USA, 21–25 October 2019

2. Sippel, M., Klevanski, J., Kauffmann, J.: Innovative method for return to the launch site of reusable winged stages. In: International Astronautical Congress. 52nd International Astronautical Congress, Toulouse, France, 1–5 October 2001

3. Stappert, S., Wilken, J., Bussler, L., Sippel, M.: A systematic comparison of reusable first stage return options. 8th European Conference on Aeronautics and Space Sciences (EUCASS), Madrid, Spain, 1–4 July 2019

4. Sippel, M., Bussler, L., Krause, S., Cain, S., Stappert, S.: Bringing highly efficient RLV-return mode "In-air capturing" to reality. HiSST 2018, Moscow, Russia, 26–29 November 2018

5. Sippel, M., Singh, S., Stappert, S.: RLV-Return Mode "In-Air-Capturing" and Definition of its Development Roadmap. 9th European Conference on Aeronautics and Space Sciences (EUCASS), Lille, France, 27 June–01 July 2022

6. Patentschrift (patent specification) DE 101 47 144 C1, Verfahren zum Bergen einer Stufe eines mehrstufigen Raumtransportsystems, released 2003

7. Krause, S., Cain, S., Funke, A., Ferrándiz, M., González, J.: Overview of demonstrators and planned flight operations of a scaled in-air capturing demonstration, 9th European Conference on Aeronautics and Space Sciences (EUCASS), Lille, France 27 June–01 July 2022

8. Stappert, S., Wilken, J., Dominguez G. J. C., Sippel, M.: Evaluation of Parametric Cost Estimation in the Preliminary Design Phase of Reusable Launch Vehicles, 9th European Conference on Aeronautics and Space Sciences (EUCASS), Lille, France, 27 June - 01 July 2022

9. Callsen, S., Stappert, S., Sippel, M.: Study on future European winged reusable launchers, 9th European Conference for Aeronautics and Space Sciences (EUCASS), Lille, France, 27 June–01 July 2022

10. Stappert, S., Sippel, M., Callsen, S., Bussler, L.: Concept 4: A Reusable Heavy-Lift Winged Launch Vehicle using the In-Air-Capturing method, 2nd International Conference on High-Speed Vehicle Science Technology (HiSST), Bruges, Belgium, 11 - 15 September 2022

11. Kucukosman, Y. C., Lopes, S., Buckingham., S., Planquart, P., Singh, S., Bussler, L., Stappert, S., Sippel, M.: Aerodynamic characterization of in-air capturing vehicles using CFD simulations, 9th Conference on Aeronautics and Space Sciences (EUCASS), Lille, France, 27 June – 01 July 2022

12. Singh, S., Stappert, S., Buckingham., S., Lopes, S., Kucukosman, Y. C., Simioana, M., Pripasu, M., Wiegand, A., Sippel, M., Planquart, P.: Dynamic modelling and control of an aerodynamically controlled capturing device for 'In-Air Capturing' of a Reusable Launch Vehicle, 11th International ESA Conference on Guidance, Navigation and Control Systems, 2021, online

13. Singh, S., Simioana, M.: Full scale simulation of in-air capturING. VKI Lecture Series, Sint-Genesis-Rode, Belgium, 25–27 April 2022

14. Singh, S., Bussler, L., Callsen, S., Stappert, S., Lopes, S., Buckingham, S.: A superposition approach to aerodynamic modelling of a capturing device used for in-air capturing of a reusable launch vehicle, 9th European Conference on Aeronautics and Space Sciences (EUCASS), Lille, France, 27 June–01 July 2022

15. Singh, S., Stappert, S., Bussler, L., Sippel, M., Kucukosman, Y. C., Buckingham, S.: A full-scale simulation and analysis of formation flight during in-air capturing, 72nd International Astronautical Congress (IAC), Dubai, United Arab Emirates, 25–29 October 2021

16. Singh, S., Simioana, M., Stappert, S., Sippel, M., Buckingham, S., Lopes, S., Kucukosman, Y. C.: Control design and analysis of a capturing device performing in-air capturing of a reusable launch vehicle, 9th European Conference on Aeronautics and Space Sciences (EUCASS), Lille, France, 27 June–01 July 2022

17. Singh, S., Stappert, S., Bussler, L., Sippel, M., Kucukosman, Y.C., Buckingham, S.: Full-scale simulation and analysis of formation flight during In-Air Capturing of a winged reusable launch vehicle. Journal of Space Safety Engineering **9**(4), 541–552 (2022)

18. Singh, S., Bussler, L., Stappert, S., Sippel, M., Kucukosman, Y. C., Buckingham, S.: Simulation and analysis of pull-up maneouvre during in-air capturing of a reusable launch vehicle, 9th European Conference on Aeronautics and Space Sciences (EUCASS), Lille, France, 27 June–01 July 2022